



Measurement of ρ , the Ratio of the Real to Imaginary Part of the
 $\bar{p}p$ Forward Elastic Scattering Amplitude, at $\sqrt{s} = 1.8$ TeV

The E710 Collaboration

N. Amos (a), C. Avila (a), W. Baker (a), M. Bertani (b)(2), M. Block (c), D. Dimitroyannis (d)(3),
D. Eartly (a), R. Ellsworth (e), G. Giacomelli (b), B. Gomez (a)(4), J. Goodman (d), C. Guss (c)(5),
A. Lennox (a), M. Mondardini (b)(6), J. Negret (a)(4), J. Orear (f), S. Pruss (a), R. Rubinstein (a),
S. Sadr (c), J. Sanabria (a), S. Shukla (a), M. Spagnoli (b), I. Veronesi (b), and S. Zucchelli (b)

^(a) *Fermi National Accelerator Laboratory, Batavia, Illinois 60510*

^(b) *Universita' di Bologna and Istituto Nazionale di Fisica Nucleare, Bologna, Italy*

^(c) *Northwestern University, Evanston, Illinois 60201*

^(d) *University of Maryland, College Park, Maryland 20742*

^(e) *George Mason University, Fairfax, Virginia 22030*

^(f) *Cornell University, Ithaca, New York, 14853*

October 1991

* Submitted to *Physical Review Letters*.



Measurement of ρ , the Ratio of the Real to Imaginary Part of the $\bar{p}p$ Forward Elastic Scattering Amplitude, at $\sqrt{s} = 1.8$ TeV

N. A. Amos^(a), C. Avila^{(a)(1)}, W. F. Baker^(a), M. Bertani^{(b)(2)}, M. M. Block^(c), D. A. Dimitroyannis^{(d)(3)}, D. P. Eartly^(a), R. W. Ellsworth^(e), G. Giacomelli^(b), B. Gomez^{(a)(4)}, J. A. Goodman^(d), C. M. Guss^{(c)(5)}, A. J. Lennox^(a), M. R. Mondardini^{(b)(6)}, J. P. Negret^{(a)(4)}, J. Orear^(f), S. M. Pruss^(a), R. Rubinstein^(a), S. Sadr^(c), J. C. Sanabria^(a), S. Shukla^(a), M. Spagnoli^(b), I. Veronesi^(b), and S. Zucchelli^(b)

(The E-710 Collaboration)

- (a) Fermi National Accelerator Laboratory, Batavia, Illinois 60510
- (b) Universita' di Bologna and Istituto Nazionale di Fisica Nucleare, Bologna, Italy
- (c) Northwestern University, Evanston, Illinois 60201
- (d) University of Maryland, College Park, Maryland 20742
- (e) George Mason University, Fairfax, Virginia 22030
- (f) Cornell University, Ithaca, New York 14853

ABSTRACT

We have measured ρ , the ratio of the real to the imaginary part of the $\bar{p}p$ forward elastic scattering amplitude, at $\sqrt{s} = 1.8$ TeV. A previous measurement at $\sqrt{s} = 546$ GeV had been interpreted as inconsistent with the expected value based on lower energy data and dispersion relations; new physics phenomena had been frequently invoked to explain the apparent discrepancy. Our result, $\rho = 0.140 \pm 0.069$, is consistent with the expected behavior, and thus no new physics is required.

As part of our study of $\bar{p}p$ interactions at the Fermilab Tevatron Collider, we report here a measurement of ρ , the ratio of the real to imaginary part of the forward $\bar{p}p$ elastic scattering amplitude, at $\sqrt{s} = 1.8$ TeV. Due to the analyticity of the elastic scattering amplitude, a determination of ρ together with measurements of pp and $\bar{p}p$ total cross sections and some very general assumptions about the scattering amplitude, allows the behavior of total cross sections to be determined at much higher energies than are currently available.

Fits to ρ and σ_T available up to ISR energies have been used in the above manner to predict values of ρ and σ_T at SPS and Tevatron Collider energies.^(1,2) The predictions for total cross sections were in agreement with measured values when they became available. However the SPS UA4 measurement⁽³⁾ at $\sqrt{s} = 546$ GeV of $\rho = 0.24 \pm 0.04$, was ~ 2.5 standard deviations from the expected value of ~ 0.14 . This possible discrepancy was discussed in many theoretical papers; some examples are given in References 4-9. There was a general consensus in these papers that some new physics was needed to accommodate a value of 0.24; predictions were given for σ_T and ρ at $\sqrt{s} = 1.8$ TeV, although some of the predictions were not consistent with our subsequent measurement⁽¹⁰⁾ of σ_T at $\sqrt{s} = 1.8$ TeV.

Our apparatus has been described in earlier publications⁽¹⁰⁻¹³⁾, to which reference can be made for details. In order to measure ρ , measurements of the

elastic scattering $\frac{d\sigma}{dt}$ have to be made to very small $|t|$ values, around the t value where the maximum interference between coulomb and nuclear scattering occurs. At our energy, this is at $|t| \approx 0.001$ (GeV/c)² which corresponds to a scattering angle of only 35 μ r. Using the detectors in our outer "Roman Pots" (see Figure 1 of Reference 11), we were able to measure elastic scattering down to these angles.

This measurement includes the same data as in our previously reported results, but with two additions. The first is that some more runs were analyzed, increasing the total integrated luminosity by almost 75%. The second is that we analyzed events in our detectors to within 2.75 mm of the beam center (the chamber extended down to 2.2 mm from the beam center). This allowed us to measure scattering at small enough $|t|$ values to obtain ρ , although background rates were large close to the beam. Data were analyzed over the range $0.001 \leq |t| \leq 0.14$ (GeV/c)², and our final sample contained 180,000 elastic events.

Event selection has been described in our earlier publications. Because the drift chamber horizontal (x) coordinate readouts (based on charge division) were known with substantially less accuracy than the vertical (y) coordinate readouts, we integrated over x and only used the y coordinate in our analysis. Although each bin in y , after integrating over x , then covers a range of t values, it can be shown analytically that ρ can be obtained correctly from the data; this was also verified by Monte Carlo studies. There is some loss of statistical accuracy using this method, but it avoids the systematic uncertainties which would have been present in the result due to our x readout uncertainties. Note that the ends of the x integration are the precisely known edges of the trigger counters.

Elastic events were obtained from detectors in conjugate pot pairs BC or AD in the schematic arrangement shown in Figure 1a. Figure 1b shows for one run a scatter plot of the correlation for each event between the y coordinates of the detectors in pots AD; the elastic events can be clearly seen as the diagonal band, together with background close to the beam in either pot. To obtain backgrounds we used the non-conjugate pot pairs AC and BD. For example, the background in the AD combination was obtained from simultaneous data taken of the combinations AC (for detector A) and BD (for detector D). These two distributions were then combined to produce the AD background distribution shown in Figure 1c. We would expect that the background is due to uncorrelated hits in the chambers caused by, for example, beam halo, which is known to increase sharply close to the beam. The correlated background due to inelastic events is small, since the ~ 100 m of 4T magnetic field between the interaction point and either detector limits particles reaching the detectors to be within $\sim 1\%$ of the circulating beam momentum. Extensive studies showed that the shape of the distribution in Figure 1c is identical to that of the background in Figure 1b, as expected. The background obtained in this way was normalized to that in the conjugate pot distribution combinations outside the elastic region, and subtracted bin by bin. In some runs the background at our lowest y (vertical distance from beam center) bin was almost equal to the signal, although it dropped by a factor of 10 in 2.75 mm. However, using the method described above, the background was determined even in the worst case to an accuracy of $\pm 3\%$.

We use the following expression for the elastic differential cross section.

$$\frac{1}{L} \frac{dN_{el}}{dt} = \frac{d\sigma}{dt} = \frac{4\pi\alpha^2(\hbar c)^2 G^4(t)}{|t|^2} + \frac{\alpha(\rho - \alpha\phi)\sigma_T G^2(t)}{|t|} \exp(-B|t|/2) + \frac{\sigma_T^2(1+p^2)}{16\pi(\hbar c)^2} \exp(-B|t|) \quad (1)$$

The three terms in equation (1) are due to, respectively, coulomb scattering, coulomb-nuclear interference, and nuclear scattering. L is the integrated

accelerator luminosity; $\frac{dN_{el}}{dt}$ is the observed elastic differential distribution; α is the fine structure constant, ϕ is the relative coulomb-nuclear phase, given by (14) $\ln(0.08|t|^{-1} - 0.577)$; G(t) is the nucleon electromagnetic form factor, which we parameterize in the usual way as $(1 + |t|/0.71)^{-2}$. [t is in (GeV/c)²]

We also use the following two equations:

$$\sigma_i^2 = \frac{1}{L} \frac{16\pi(\hbar c)^2}{(1+p^2)} \left. \frac{dN_{el}^n}{dt} \right|_{t=0} \quad (2)$$

$$\sigma_T = \frac{1}{L} (N_{el}^n + N_{inel}) \quad (3)$$

Equation (2) is obtained from the optical theorem. N_{el}^n is the total number of nuclear elastic events, obtained from the observed $\frac{dN_{el}}{dt}$ distribution in the t region where nuclear scattering dominates, and extrapolated to $t = 0$ and $t = \infty$ using the

form $\exp(-B|t|)$. $\left. \frac{dN_{el}^n}{dt} \right|_{t=0}$ is the observed differential number of nuclear elastic events extrapolated to $t = 0$ using the same form. N_{inel} is the total number of inelastic events; our method for obtaining this, using detectors close to the interaction point, has been described earlier⁽¹⁰⁾. Note that equations (2) and (3)

allow us to express L in terms of σ_T and ρ . Then $\frac{dN_{el}}{dt}$ in equation (1) can be expressed in terms of just 3 unknowns: σ_T , B and ρ . Our input data are our

measurements of $\frac{dN_{el}}{dt}$ together with the total number of inelastic events, N_{inel} , for the same runs as for the elastic data. We do a least squares analysis for σ_T , B and ρ in equation(1) using all our input data. As explained earlier, this procedure was modified in practice, although not in principle, because instead of

using measurements of $\frac{dN_{el}}{dt}$ as input, we used $\frac{dN_{el}}{dy}$ where y is the vertical distance from the beam center, and where each y bin covers a specified range of t .

The result obtained from the 3-parameter least squares fit is

$$\begin{aligned}\rho &= 0.140 \pm 0.069 \\ B &= 16.99 \pm 0.47 \text{ (GeV/c)}^2 \\ \sigma_T &= 72.8 \pm 3.1 \text{ mb}\end{aligned}$$

The analysis procedure has been designed so that the errors are almost totally statistical. The χ^2 per degree of freedom of the fit is 1.3.

The values of B and σ_T given above are consistent, within the quoted errors, with our earlier values^(10,12,13), and supersede them. None of our earlier

physics conclusions is substantially altered. We show in Figure 2 all of our $\frac{dN_{el}}{dy}$ data as a function y^2 , together with our fit. Figure 3a shows the same data in the small y region, together with our fit and two curves showing the effect of changing ρ , but keeping B and $\sigma_T(1+\rho^2)$ fixed. [Note that B and $\sigma_T(1+\rho^2)$ are essentially determined from the larger y data]. Figure 3b, with data in the small y region, shows more explicitly how much our data differ from values of ρ of 0 and

0.28. We note again that the figures show $\frac{dN_{el}}{dy}$ with each y bin corresponding to a

range of t ; for example, our smallest y bin covers the range $0.00095 \leq |t| \leq 0.0777$ $(\text{GeV}/c)^2$, and our largest covers $0.0651 \leq |t| \leq 0.1431$ $(\text{GeV}/c)^2$.

We have verified that our result for ρ is stable when we change the lowest y of the data used in the fit from 2.75mm to 4.25mm from the beam center. Since backgrounds in our data are reduced by a factor of ~ 3 in that y range, this gives us confidence in our background subtraction technique. The result is also constant over four data sets taken from our two data-taking runs which were separated by about a month.

Our result for ρ is shown in Figure 4, together with results at lower energies^(3,15,16), and a curve⁽¹⁷⁾ showing the prediction based on previously existing pp and $\bar{p}p$, σ_T and ρ data except for the ρ value at $\sqrt{s} = 546$ GeV. It can be seen that our value of ρ is consistent with that expected, and thus our result does not require the addition of any new physics.

This work was supported by the U.S. Department of Energy, the U.S. National Science Foundation, the Italian Ministero Pubblica Istruzione and the North Atlantic Treaty Organization.

REFERENCES

- (1) Present address: University of Massachusetts, Amherst, Massachusetts
 - (2) Present address: University of Ferrara, Ferrara, Italy
 - (3) Present address: Northwestern University, Evanston, Illinois
 - (4) Present address: Universidad de Los Andes, Bogota, Colombia
 - (5) Present address: Temple University, Philadelphia, Pennsylvania
 - (6) Present address: Cornell University; mailing address: CERN, Geneva, Switzerland
1. U. Amaldi et al., Phys Lett B66, 390 (1977)
 2. M. M. Block and R. N. Cahn, Phys Lett B149, 245 (1984); Rev Mod Phys 57, 563 (1985)
 3. D. Bernard et al., Phys Lett B 198, 583 (1985)
 4. E. Leader, Phys Rev Lett 59, 1525 (1987)
 5. D. Bernard, P. Gauron and B. Nicolescu, Phys Lett B199, 125 (1987)
 6. P. M. Kluit, Phys Lett B222, 155 (1989)
 7. K. Kang and A. R. White Phys Rev D42, 835 (1990) and Phys Lett B266, 147 (1991)
 8. A. Donnachie and P. V. Landshoff, Particle World 2, 7 (1991)
 9. S. Barshay, P. Heiliger and D. Rein, Preprint PITHA 91/5 (1991)
 10. N. A. Amos et al., Phys Lett B243, 158 (1990)
 11. N. A. Amos et al., Phys Rev Lett 61, 525 (1988)
 12. N. A. Amos et al., Phys Rev Lett 63, 2784 (1989)
 13. N. A. Amos et al., Phys Lett B247, 127 (1990)
 14. G. B. West and D. R. Yennie, Phys Rev 172, 1413 (1968)
 15. L. Fajardo et al., Phys Rev D24, 46 (1981)
 16. N. A. Amos et al., Nucl Phys B262, 689 (1985)
 17. See Reference 2. The curve shown is taken from a later version, M. M. Block et al., Phys Rev D41, 978 (1990)

FIGURE CAPTIONS

- Figure 1a. Schematic side view of the experiment, with detectors in the four pots A,B,C,D.
- Figure 1b. Scatter plot of the correlation for each event between the y coordinates in the detectors in pots A and D, for one run.
- Figure 1c. Scatter plot of background events in pots A and D, corresponding to the data of Figure 1b; see text for details.
- Figure 2. Results of this experiment for the elastic scattering distribution dN/dy vs y^2 , for almost all of the data. The best fit curve described in the text is shown.
- Figure 3a. As for Figure 2, with only data for $y^2 < 210 \text{ mm}^2$. The solid curve is the best fit described in the text ($\rho = 0.140$); the long-dashed and short-dashed curves show values of ρ of 0.280 and 0, respectively (see text for details).
- Figure 3b. The same data as in Figure 3a, given in a form to show the deviation of the data and the best fit ($\rho = 0.140$) from $\rho = 0$ (horizontal line) and $\rho = 0.28$ (dashed curve).
- Figure 4. Our result for ρ , together with results from lower energies (References 3, 15, 16), and a curve (Reference 17) showing the prediction based on existing pp and $\bar{p}p$, σ_T and ρ data except for the ρ value at $\sqrt{s} = 546 \text{ GeV}$.

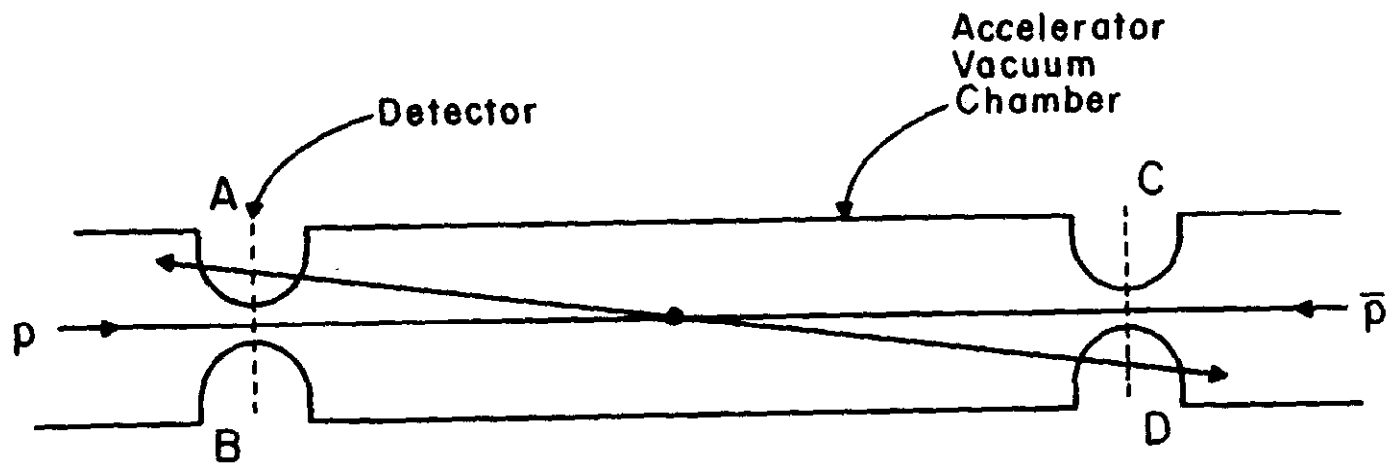
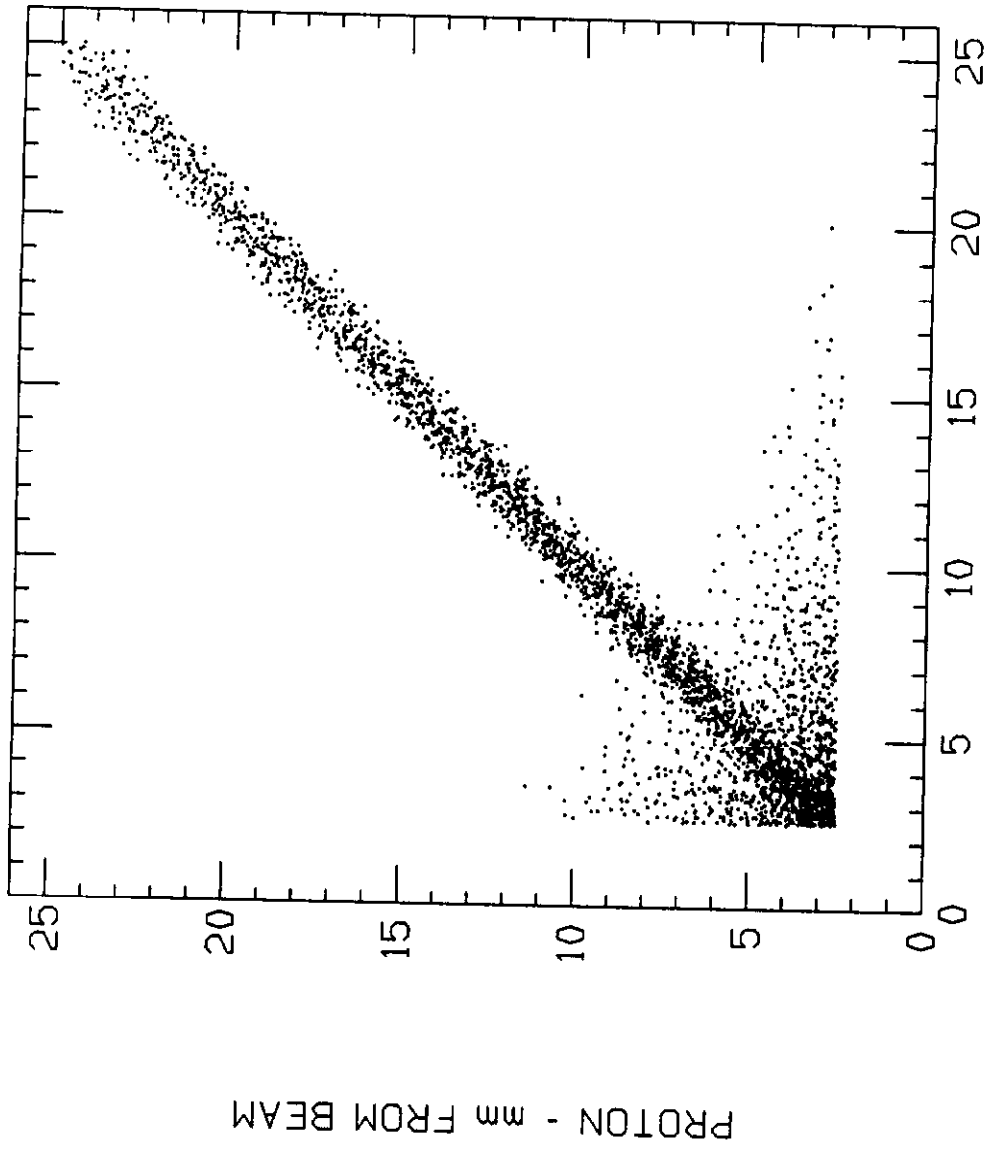
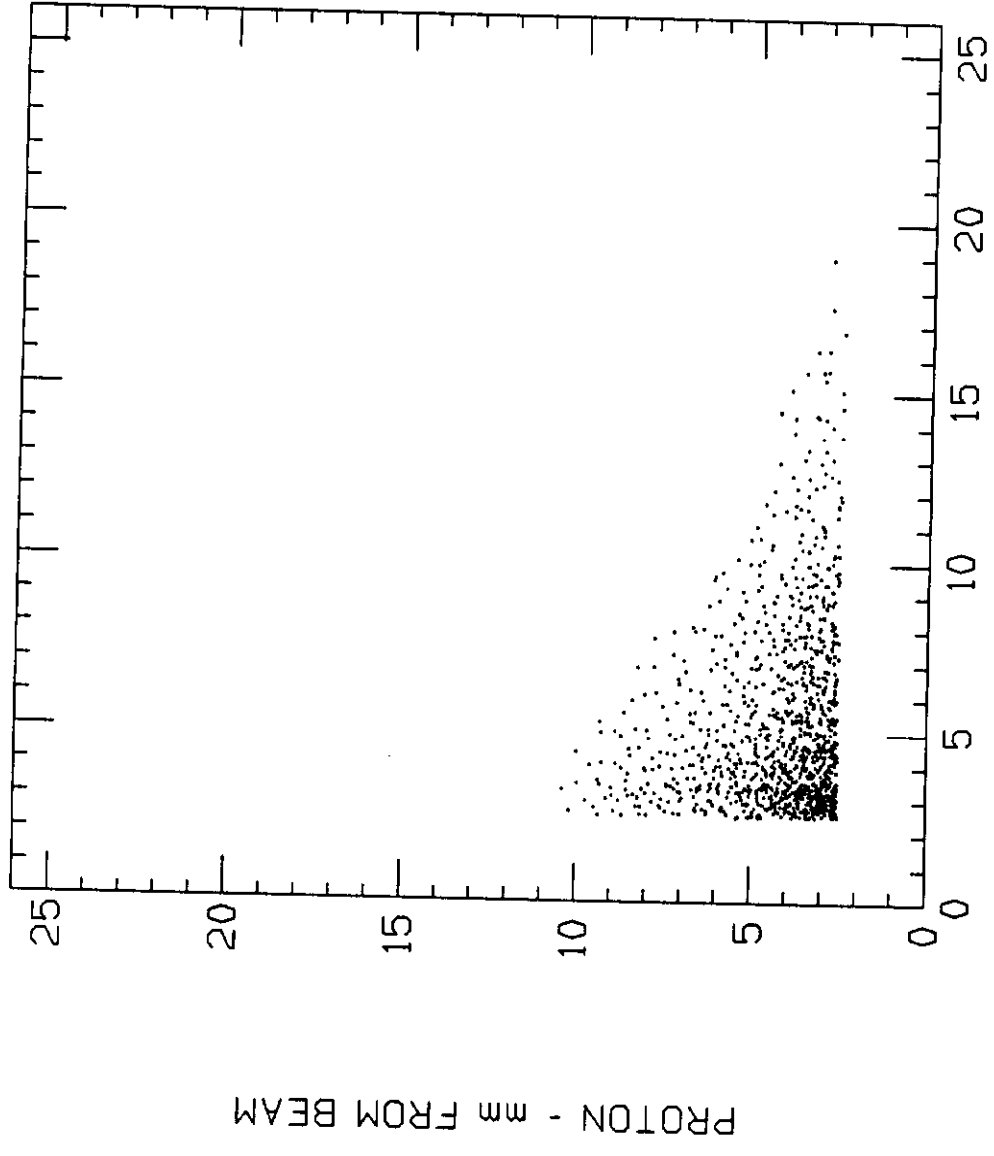


Figure 1a



ANTIPROTON - mm FROM BEAM



ANTIPROTON - mm FROM BEAM

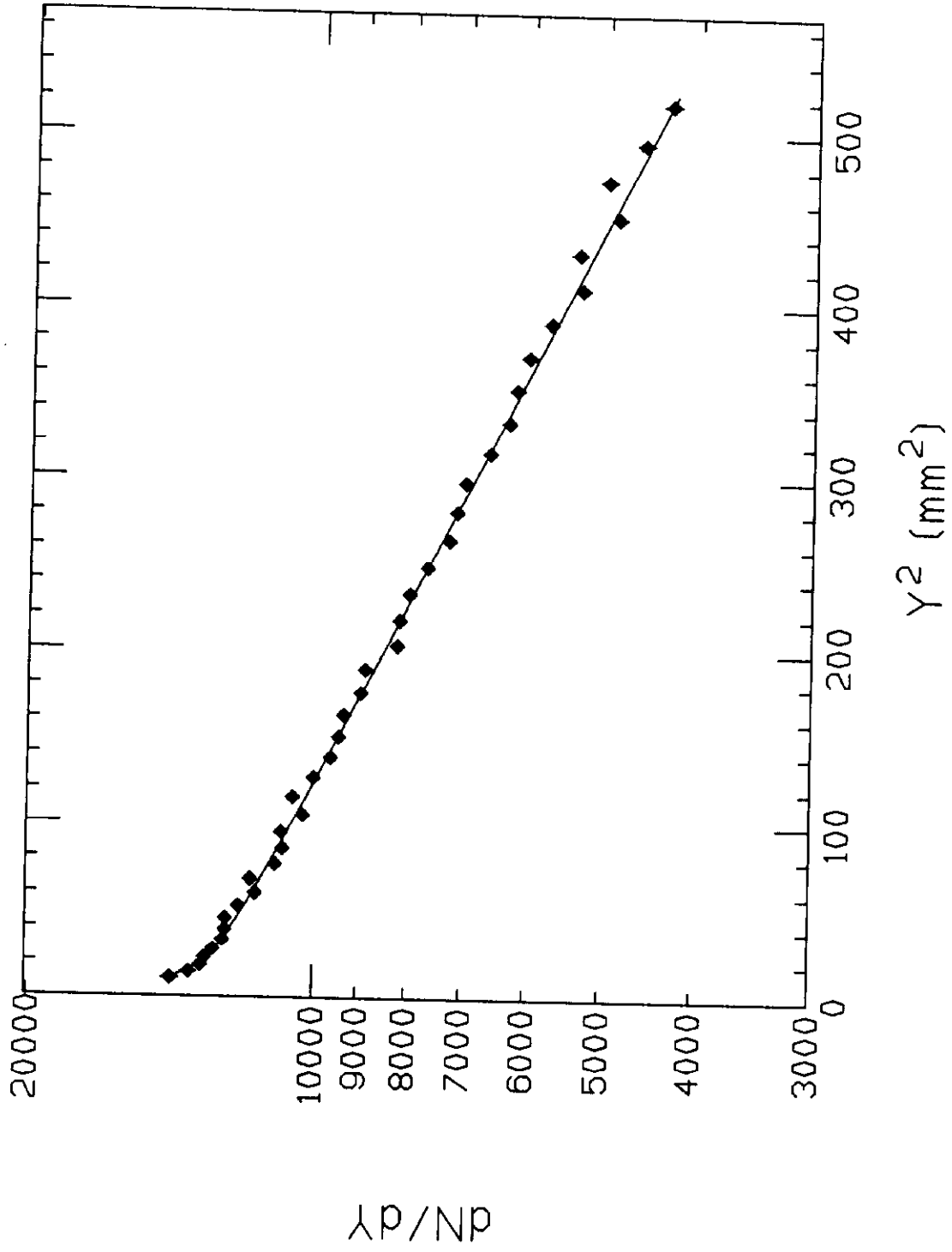


Figure 2

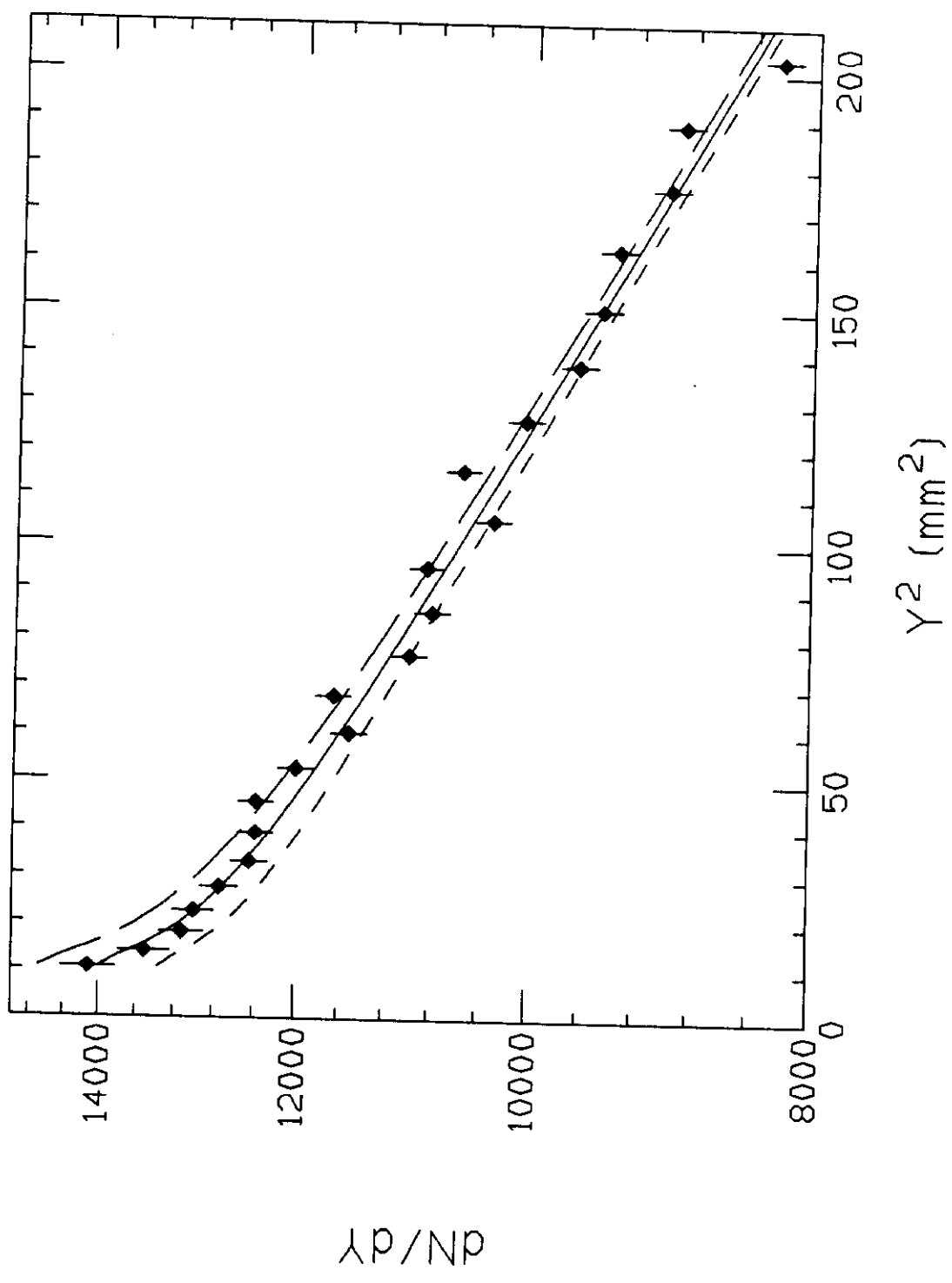


Figure 3a

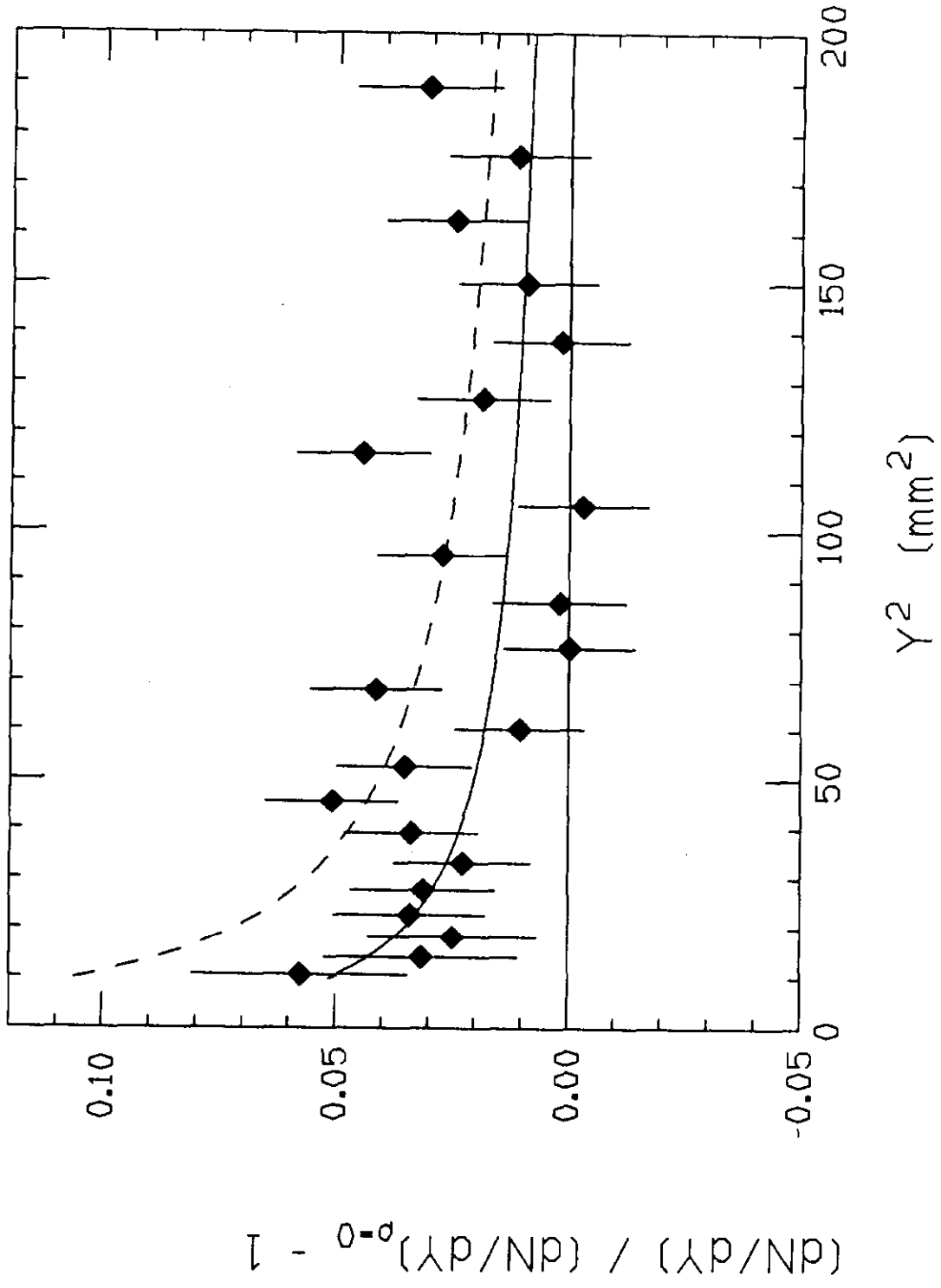


Figure 3b

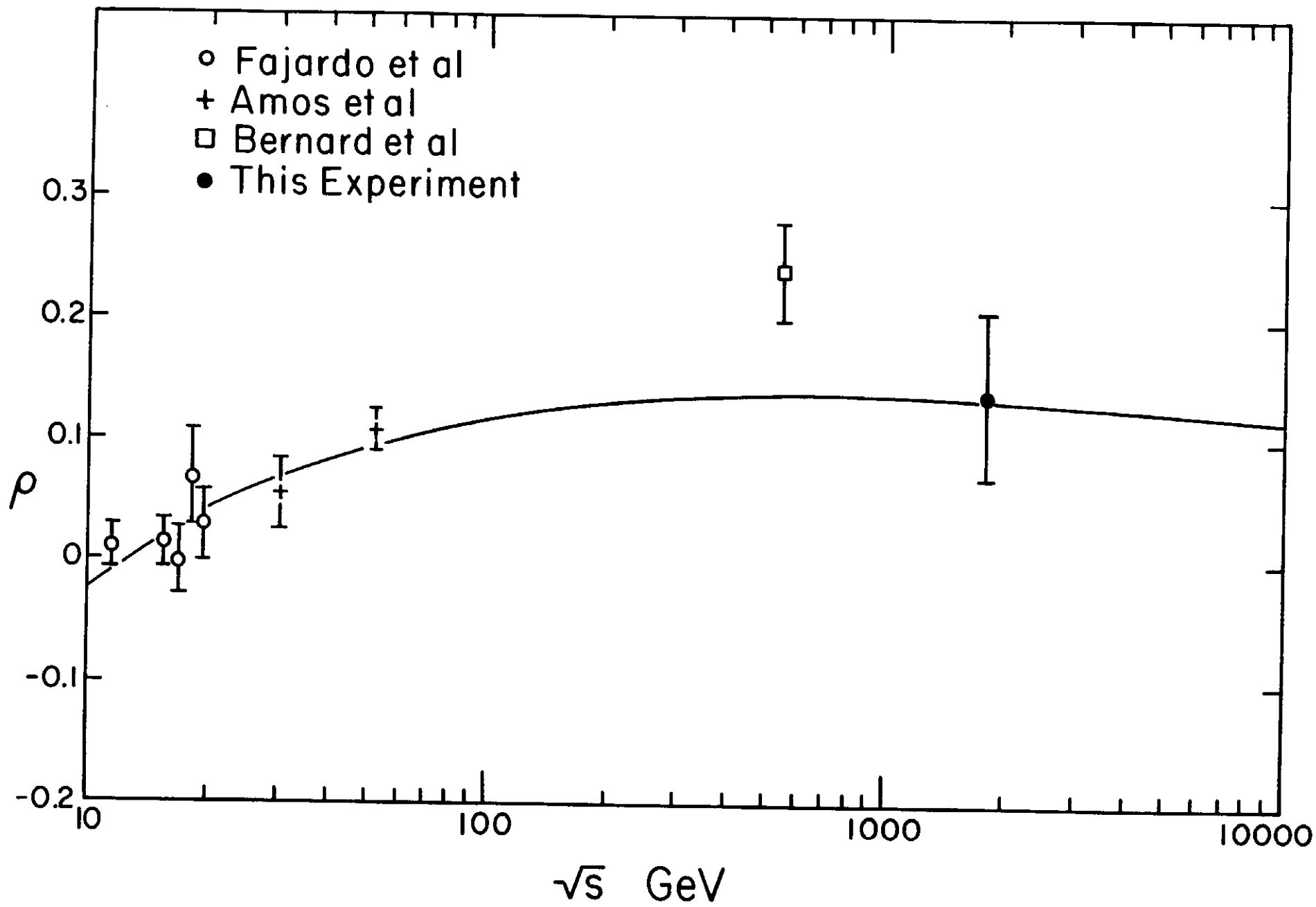


Figure 4